# Thermochemical remanent magnetization in Precambrian rocks: Are we sure the geomagnetic field was weak?

A. V. Smimov and J. A. Tarduno
Department of Earth and Environmental Sciences, University of Rochester, Rochester, New York, USA

Received 20 September 2004; revised 7 January 2005; accepted 21 March 2005; published 30 June 2005.

[i] Thellier paleointensity determinations from two dikes of the Early Proterozoic (~2.46 Ga) Matachewan dike swarm (Canada) yield field values of 2.14 ± 0.18 and 9.81 ± 1.65 microT. Corresponding values of virtual axial dipole moment are very low (0.54 ± 0.05 x $10^{22}$ and 2.49 ± 0.42 x $10^{22}$ Am$^2$, respectively) when compared with the modern field. The characteristic remanent magnetization (ChRM) was isolated over a narrow range of high unblocking temperatures (~520-580°C). Detailed rock magnetic analyses indicate that the ChRM is carried by nearly stoichiometric pseudo single domain magnetite. Scanning electron microscopy (SEM) reveals that the magnetite is in the form of fine intergrowths with ilmenite, formed by oxyexsolution during cooling. The high-temperature oxidation defined in the SEM images could have continued at temperatures below the Curie point of magnetite. In this case, the ChRM would be a thermochemical remanent magnetization (TCRM) rather than a thermal remanent magnetization (TRM). Estimates of the TCRM/TRM ratio show that the Thellier data could underestimate the true field value by a factor of 4 without violating experimental selection criteria. This uncertainty in TRM fidelity translates into a potential range of field values that spans that defined by the modern field (~8 x $10^{22}$ Am$^2$) and proposed low Precambrian levels (~2 x $10^{22}$ Am$^2$). Therefore understanding further how TCRM is acquired and records the field represents a major challenge if these and many other similar rocks are to be used in Thellier studies aimed at defining the strength of the Precambrian field.

**Citation:** Smirnov, A. V., and J. A. Tarduno (2005), Thermochemical remanent magnetization in Precambrian rocks: Are we sure the geomagnetic field was weak?, *J. Geophys. Res., 110,* B06103, doi:10.1029/2004JB003445.

## 1. Introduction

[2] The long-term history of geomagnetic field strength may provide crucial insight into the evolution of the geodynamo. For example, some thermal models predict the onset of the modem compositionally driven geodynamo [e.g., *Hollerbach and Jones,* 1993; *Labrosse and Macouin,* 2003] and growth of the inner solid core [e.g., *Labrosse etal,* 2001; *BrodholtandNimmo,* 2002] in the Precambrian. An attendant sharp increase in the geomagnetic field intensity has also been predicted [*Stevenson et al,* 1983; *Breuer and Spohn,* 1995; *Labrosse et al,* 1997]. In other models, the geodynamo is less sensitive to the presence of the inner core [e.g., *Wicht,* 2002].

[3] Experimental data on the strength of the Precambrian field could shed some light on these issues, but unfortunately the database is limited. Precambrian data form only ~5% of all available paleointensity values and they are characterized by an uneven temporal distribution. Moreover, few of the paleointensity values demonstrably represent the time-averaged field, and some clearly reflect alteration processes [e.g., *Yoshihara and Hamano,* 2004].


0148-0227/05/2004JB003445S09.00

[4] Notwithstanding these limitations, several authors have reported relatively low field intensities for the Precambrian [e.g., *Selkin et al.,* 2000; *Yu and Dunlop,* 2002] and some have suggested it was a general characteristic of the field [e.g., *Macouin et al.,* 2003]. Others have reported values for the Precambrian field that are consistent with present-day strengths [*Yoshihara and Hamano,* 2000; *Smirnov et al.,* 2003]. Hence, at the very least, the existing database must be supplemented with additional robust paleointensity determinations.

[5] However, significant weathering and low-grade metamorphism in many Precambrian rocks hamper paleointensity studies [e.g., *Hale,* 1987]. The Thellier technique [*Thellier and Thellier,* 1959], arguably the most reliable method of paleointensity determination, often fails on such altered rocks because of mineralogical changes induced by the successive heating steps required by the method.

[6] To identify experimental alteration, a set of reliability criteria has been developed on the basis of the characteristics of the natural remanent magnetization (NRM) and thermoremanent magnetization (TRM) data [e.g., *Coe et al.,* 1978], In some cases the data may not be free of alteration effects [e.g., *Tanaka and Kono,* 1991; *Calvo et al.,* 2002; *Yamamoto et al.,* 2003], so additional tests based on

independent rock magnetic data have been proposed [e.g., *McElhinny and Evans*, 1968; *Haag et al.*, 1995; *Smirnov and Tarduno*, 2003].

[7] Yet, even these additional tests may be insufficient to insure that the experimentally defined field value faithfully reproduces the past field. The starting point of Thellier analyses is TRM, and it is not always clear that the magnetization of some Precambrian rocks has this origin.

[8] In this paper, we report paleointensity results obtained from two dikes of the Early Proterozoic (~2.46 Ga) Matachewan dike swarm of the Superior province, Canada. The paleointensity study is accompanied by analyses of magnetic mineralogy. On the basis of these results we discuss the possibility that the rocks carry a thermochemical remanent magnetization rather than a true TRM, which ultimately leads to the false impression that the Precambrian geomagnetic field was weak.

## 2. Background Geology and Sampling

[9] The Matachewan dike swarm radiates up to 700 km north and northwest from a broad focal region near Lake Huron and covers about 250,000 km$^2$ of the central Superior province. *Heaman* [1997] reported two U-Pb ages for the swarm ($2473^{+16}_{-9}$ Ma and 2446 ± 3 Ma) based on baddeleyite and zircon fractions. Emplacement of the dikes has been associated with mantle plume activity [*Halls and Bates*, 1990] or failed rifting [*Fahrig*, 1987]; these different models are reflected in the end-member solutions of the current debate on the origin of global large igneous provinces [*Anderson*, 2003; *Foulger and Natland*, 2003; *Sleep*, 2003].

[10] The dikes are olivine-rich to quartz iron-rich tholeiites, varying from ~1 to >50 m in width [*Ernst and Halls*, 1984]. The dikes have experienced no more than lower greenschist facies hydrous metamorphism [e.g., *Bates and Halls*, 1991; *Phinney and Halls*, 2001].

[11] There is no significant variation in the mineralogy and texture of the dikes [e.g., *Ernst and Halls*, 1984]. However, significant trace element variations that do not correlate with terrane lithologies were observed and interpreted to reflect a two-stage process of dike emplacement [e.g., *Condie et al.*, 1987; *Nelson et al.*, 1990]. Initial fractional crystallization and assimilation took place in the lower crust. Subsequently, the evolved magmas were periodically transported to shallow (10–15 km) magma chambers where further fractional crystallization occurred [*Nelson et al.*, 1990; *Phinney and Halls*, 2001].

[12] The Matachewan swarm is cut by the Kapuskasing structural zone (KSZ), a northeast trending fault-bounded belt of uplifted Archean middle to lower crust, marked by positive gravity and magnetic anomalies [e.g., *Manson and Halls*, 1997]. While the age of KSZ uplift is uncertain, it clearly postdates dike emplacement [e.g., *Halls et al.*, 1994].

[13] Extensive paleomagnetic study of the Matachewan swarm [e.g., *Schutts and Dunlop*, 1981; *Halls and Bates*, 1990; *Symons et al.*, 1994; *Halls and Zhang*, 1998] has provided important constraints on the tectonic history of the Superior province in the Proterozoic [e.g., *Bates and Halls*, 1991; *Halls and Zhang*, 2003]. Only a single geomagnetic reversal has been found; a structural model controlled by field mapping and the presence of clouded feldspar [*Poldervaart and Gilkey*, 1954] suggests the reversal reflects different depths of the crust in which the dikes were intruded [*Bates and Halls*, 1991; *Halls*, 1991]. Specifically, the KSZ exposes deeper crustal layers. Dikes from these lower layers are thought to have resided at elevated temperatures for a longer period of time, allowing greater exsolution of Fe oxides in plagioclase feldspars. More recently, the Matachewan dikes (outside the KSZ) have been used for paleointensity studies [*Macouin et al.*, 2003; *Halls et al.*, 2004].

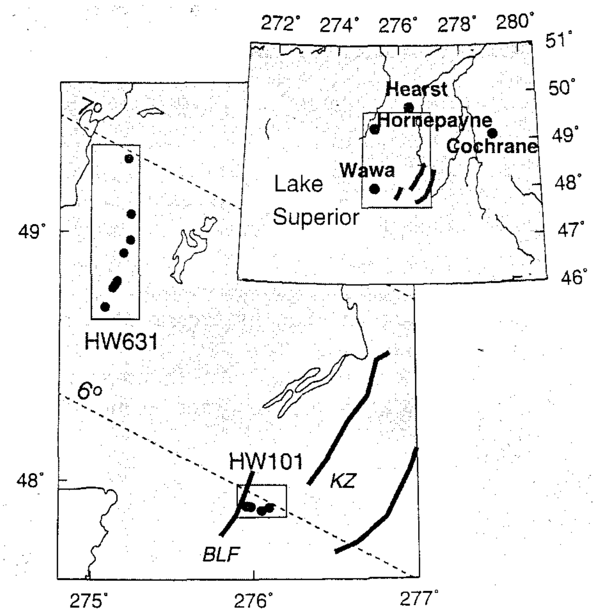


**Figure 1.** Locations of the Matachewan dikes sampled (solid circles). Boxes show two groups of dikes sampled along highway 101 (HW101) and highway 631 (HW631). GPS site coordinates are given by *Smirnov and Tarduno* [2004]. Thick solid lines show Kapuskasing structural zone (KZ) and Budd Lake fault zone (BLF). Dashed lines are ~2.46 Ga paleolatitudes calculated from the Matachewan reference pole [*Bates and Halls*, 1990] with polarity interpretation discussed by *Halls* [1998]. Inset shows the sampling area in a larger geographical context.

[14] We sampled twenty Matachewan dikes for paleomagnetic and paleointensity study (Figure 1). Ten sites were sampled along highway 101 west of the KSZ. The other ten sites were sampled further to the northwest along highway 631. A detailed description of the sampling is provided elsewhere [*Smirnov and Tarduno*, 2004].

[15] Initially we hoped that these dikes would yield plagioclase feldspar samples suitable for paleointensity analyses [e.g., *Cottrell and Tarduno*, 2000]. Unfortunately, crystals meeting selection criteria are extremely rare in the dikes we sampled and were characterized by extremely low magnetic moments. In particular, few of the crystals are clear, and saussuritization is pervasive. Accordingly, we turned our efforts to an examination of whole rocks, as prior studies have found that such samples can yield results of very high technical quality [e.g., *Macouin et al.*, 2003].

[16] Paleomagnetic analysis of whole rock samples revealed two- or three-component natural remanent magnetization (NRM) [*Smirnov and Tarduno*, 2004] (see also

Table A1).[1] A viscous overprint was removed by heating to 100–150°C. An intermediate temperature component persisted to 300–550°C. The direction of this component was consistent within a dike, but differed between dikes. The intermediate component appears to be a variable overprint acquired long after the dike cooling [e.g., *Schutts and Dunlop*, 1981]. For nineteen dikes, the characteristic remanent magnetization (ChRM) was isolated above 500°C and demagnetized within a narrow temperature range. Fifteen sites yielded paleomagnetic directions coinciding with the reference Matachewan direction for the sampling regions [*Halls and Palmer*, 1990; *Bates and Halls*, 1991]. Four sites were characterized by anomalous ChRM directions and presumably reflect a different magmatic event. We also excluded another site characterized by very low NRM intensity and unstable directional behavior.

## 3. Magnetic Mineralogy

[17] At first glance, the magnetic mineralogy of the Matachewan dikes sampled seems ideal for paleointensity analysis: the high unblocking temperatures imply magnetite as the NRM carrier. A series of rock-magnetic and scanning electron microscope analyses were performed at the University of Rochester to further confirm the suitability of the dikes for paleointensity study.

### 3.1. Scanning Electron Microscopy Analysis

[18] We examined the opaque mineralogy of our samples on polished thin sections using a low-voltage high-resolution LEO 982 scanning electron microscope (SEM) equipped with an Edax Phoenix EDS system. Backscattered electron imaging was used to identify oxide grains. Over 95% of the oxide minerals present were relatively large (several hundreds of microns to >1 mm) grains, containing one or several subordinate sets of trellis type lamellae [*Haggerty*, 1991] (Figures 2a and 2b). Between the lamellae, fine (from submicron to 2–3 μm in size) intergrowths of two phases were observed (seen as brighter and darker areas (Figures 2c and 2d)). We note that *Hodych* [1996] reported a similar pattern in a SEM study of Precambrian dikes that included Matachewan samples. In some grains, ilmenite was partially (≤5% of the total volume) replaced with sphene.

[19] The compositions of the oxide grains were determined by means of energy dispersive spectrometry (EDS). Spectra were measured at a 15 kV accelerating voltage, which is optimal for excitation of the Fe K shell. Spectral data were processed using Edax SEM Quant v.3.2 software. In addition to Fe, Ti, and O, minor amounts of Mg and Al were found in some grains. Other potential impurities (such as Si, Cr and Mn) are not present in the grains, or are at extremely low trace levels.

[20] The EDS analyses showed that the bright areas in the large oxide grains are a Fe oxide phase with very low Ti content (Figure 2e). The darker phase intergrown with the Fe oxide phase is ilmenite (Figure 2f). We note that an exact measurement of the Ti content in the Fe-rich phase was not possible because of the interaction volume of the electron beam (~2 μm). Because the range of characteristic X-ray fluorescence is at least several times larger than the size of the electron beam interaction volume [*Goldstein et al.*, 1992], the Ti lines seen in the ED spectra of Fe-rich phase are likely a "contamination signal" from the surrounding ilmenite intergrowths. No hematite, rutile, or pseudobrookite was identified by the SEM/EDS analyses. Other opaque minerals in our samples were chalcopyrite ($CuFeS_2$) and pyrite ($FeS_2$). We did not observe ilmenite other than in the intergrowths with the Fe-rich phase.

### 3.2. Thermomagnetic Analysis

[21] Temperature dependences of low-field magnetic susceptibility, $\kappa(T)$, were measured upon cycling from room temperature to 700°C (in both argon and air) using an AGICO KLY 4S magnetic susceptibility meter equipped with a high-temperature furnace and a cryostat. The $\kappa(T)$ curves were also measured on heating from −192°C to room temperature both before and after the high-temperature thermomagnetic runs.

[22] For all samples, the $\kappa(T)$ curves reveal the presence of a single magnetic phase with a Curie temperature between 575–585°C (Figure 3a), consistent with magnetite as a magnetic carrier. A characteristic peak observed at −153°C, associated with the Verwey transition indicates that the magnetite is nearly stoichiometric (Figure 3b).

[23] When heated in argon, the samples show a gradual increase of $\kappa$ with a well-pronounced Hopkinson peak, followed by a sharp decrease of $\kappa$ to the Curie temperature (Figure 3a). Such a behavior is characteristic for small pseudo single domain (PSD) and single-domain (SD) magnetite grains [*Dunlop*, 1974; *Clark and Schmidt*, 1982]. On cooling, the Hopkinson peak disappears and a small bump is observed at lower (400–500°C) temperatures (Figure 3a). After heating in argon, the Verwey transition remains well pronounced, but its magnitude is somewhat reduced.

[24] When measured in air, the heating $\kappa(T)$ curves show a small bump at ~300–350°C in addition to the Hopkinson peak (Figure 3c). The high-temperature cycling in air also resulted in a decrease of the $\kappa$ measured at room temperature. As a rule, the room temperature $\kappa$ continued to decrease after repeated high-temperature runs.

[25] The Verwey transition disappears upon heating in air, even after a single high-temperature cycle (Figure 3d). This can be explained by partial maghemitization of magnetite [*Özdemir et al.*, 1993] or homogenization of the magnetite-ilmenite intergrowths upon heating to titanomagnetite [e.g., *Bogatikov et al.*, 1971].

### 3.3. Magnetic Hysteresis

[26] Magnetic hysteresis parameters (coercivity, $H_c$; coercivity of remanence, $H_{cr}$; saturation remanence, $M_{rs}$; and saturation magnetization, $M_s$) and the acquisition of the isothermal remanent magnetization (IRM) were measured using a Princeton Measurements Corporation Alternating Gradient Force Magnetometer (AGFM). The hysteresis measurements suggest a pseudo single domain magnetic carrier in our dikes [*Day et al.*, 1977] (Figures 4a and 4c), which is in agreement with our SEM observations. The saturation fields of the IRM, 0.2 to 0.4 T, are consistent with magnetite [e.g., *Dunlop and Özdemir*, 1997].

[27] Overall, our rock magnetic analyses suggest that the Fe-rich phase seen in the SEM images (Figures 2d and 2e) is represented by nearly stoichiometric magnetite. This Fe-

[1] Auxiliary material is available at ftp://ftp.agu.org/apend/jb/2004JB003445.

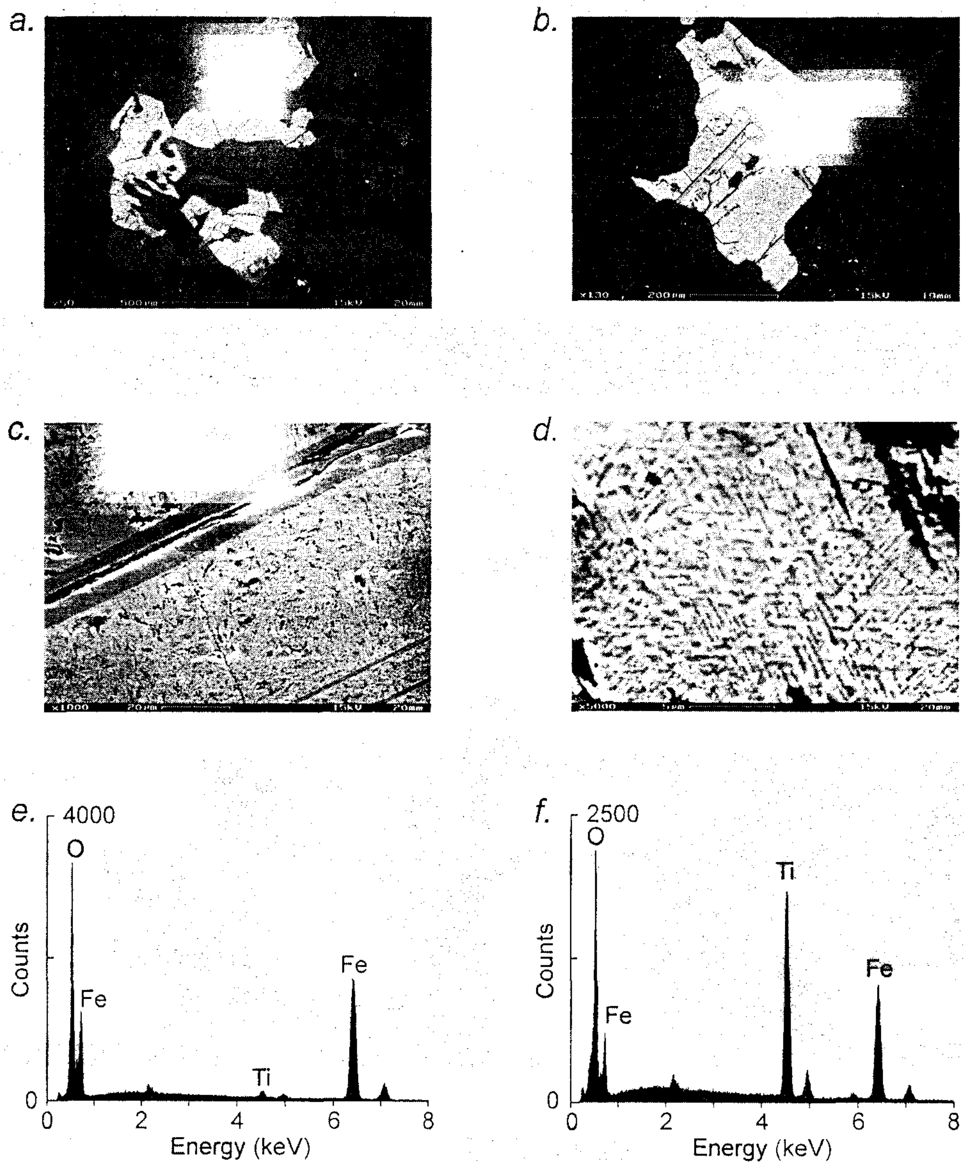


**Figure 2.** (top) Backscattered electron images of typical magnetic grains (light area) of the dikes (a) MC19 and (b) MC15. Gray and dark gray grains are the silicate matrix minerals. (middle) Close-ups showing (c) ilmenite lamellae and (d) intergrowths of low-Ti (light areas) and high-Ti (dark areas) phases between them. (bottom) Typical energy dispersive spectra from the (e) low-Ti and (f) high-Ti phases, interpreted as magnetite and ilmenite, respectively (see text).

rich phase appears to be the overwhelmingly dominant carrier of NRM in our dikes. In other Matachewan dikes, specifically those containing "clouded" feldspars, part of the whole rock NRM might be carried by magnetite exsolved in feldspar crystals.

## 4. Paleointensity Determinations

### 4.1. Experimental Technique and Results

[28] We determined paleointensity from twelve whole rock samples from sites MC-15 and MC-19 (six samples each) using the stepwise double heating Thellier method modified by *Coe* [1967]. We note that these sites record the Matachewan field direction. Magnetic remanence was measured with a 2G DC SQUID magnetometer (with a 4 cm access and a high-resolution coil geometry) at the University of Rochester. The samples were heated in an ASC TD-48 thermal demagnetization device. Temperature increments were adjusted to best record the component with high unblocking temperatures (50–400°C range, 50°C step; 400–500°C range, 20°C step; 500–600°C range, 10°C step). A laboratory field of 60 μT was used.

[29] To monitor possible alteration during the paleointensity experiment, partial thermal remanent magnetization (pTRM) checks were utilized for temperatures >450°C: after every second off-field temperature step, an on-field step at a lower temperature was measured. To be judged successful a pTRM check must fall within 5% of the

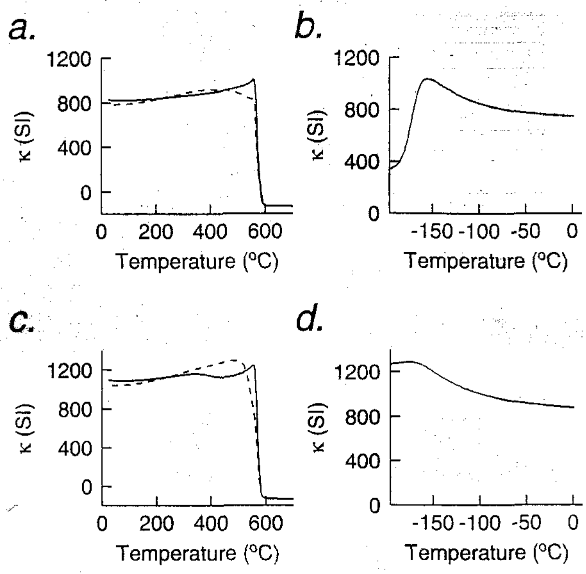


**Figure 3.** Typical dependences of low-field magnetic susceptibility (κ) versus temperature. (a) Heating (solid line) and cooling (dashed line) κ($T$) curves measured in an argon atmosphere. (b) Changes of κ upon heating from −192°C to room temperature for a fresh sample. The peak at about −153°C corresponds to the Verwey transition of magnetite. (c) Heating (solid line) and cooling (dashed line) κ($T$) curves measured in air. (d) Changes of κ upon heating from −192°C to room temperature for a sample previously heated to 700°C in air. The Verwey transition is suppressed. Measurements in argon and air were done from two specimens representing the same dike.

original TRM value. The other reliability criteria for paleointensity determination used are described elsewhere [e.g., *Cottrell and Tarduno*, 2000].

[30] For all the samples, the characteristic remanent magnetization component was isolated within a narrow range of high unblocking temperatures. The directional data for all samples used in our paleointensity experiment are presented in Table A1. The intermediate temperature component (excluded from paleointensity analysis) may be a modern field overprint in the case of dike MC19, and a mixture of Phanerozoic overprints and the primary magnetization in the case of dike MC15.

[31] All measured samples met the reliability criteria (Figure 5 and Table 1). The mean paleointensity values are 2.14 ± 0.18 (1σ) μT (MC-15) and 9.81 ± 1.65 (1σ) μT (MC-19). Corresponding values of virtual axial dipole moment are 0.54 ± 0.05 × $10^{22}$ Am$^2$ and 2.49 ± 0.42 × $10^{22}$ Am$^2$. The VADM value is calculated on the basis of the Matachewan reference pole (42°N, 58°E) from *Bates and Halls* [1990].

### 4.2. Magnetic Hysteresis Monitoring

[32] In addition to paleointensity measurements, duplicate specimens (chips) of the samples were used to study magnetic hysteresis parameters as a function of temperature. The specimens were placed in ceramic nonmagnetic boats and heated together with samples used for paleointensity determinations. Such measurements provide good monitors of possible alteration during paleointensity experiments [*Haag et al.*, 1995; *Smirnov and Tarduno*, 2003; *Riisager et al.*, 2003]. After cooling, hysteresis parameters of the duplicate samples were measured at room temperature. In addition to recording $M_s$, $M_{rs}$, $H_c$, and $H_{cr}$, we measured the total saturation magnetization ($M_s^{tot}$) before paramagnetic slope correction, and calculated the ratio between the saturation magnetization after the correction ($M_s$) and $M_s^{tot}$ to estimate a paramagnetic signal (Figure 6 and Table 2).

[33] No significant changes of the parameters measured were observed until 400°C. At higher temperatures, small changes in $M_s$ and the $M_{rs}/M_s$ ratio were observed (Figure 6b). These changes were accompanied by a monotonic increase of $H_c$ (by 35–55%) and $H_{cr}$ (by 40–60%) (Figure 6c). These changes could suggest some maghemitization induced by heating in air, or possible reversion of the magnetite-ilmenite intergrowths to titanomagnetite (possibilities first suggested by the κ($T$) data). We note that similar changes of $M_s$ and $M_{rs}/M_s$ after heating appear from the data reported by *Macouin et al.* [2003, Figure 8], but only values before and after heating were measured.

[34] To illustrate the potential experimental alteration indicated by our hysteresis data, we note that similar measurements on monitor samples of submarine basaltic

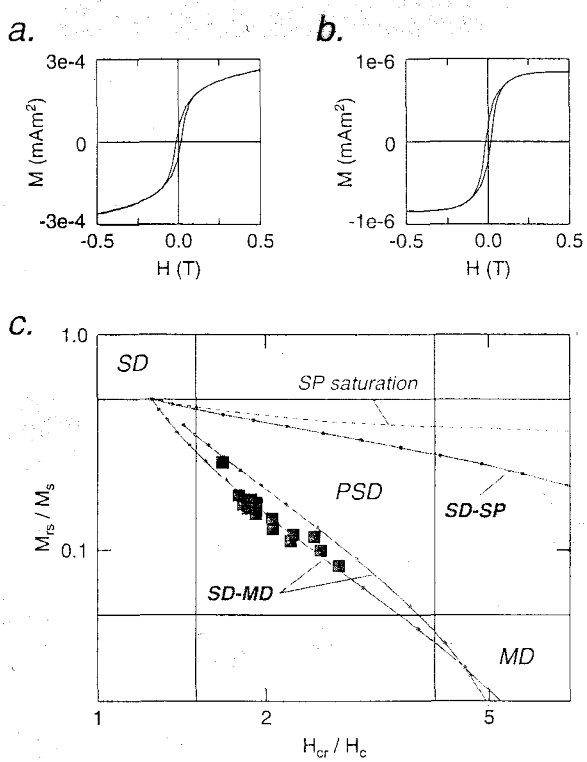


**Figure 4.** Magnetic hysteresis properties measured from 15 Matachewan dikes characterized by the Matachewan primary direction [*Smirnov and Tarduno*, 2004]. Shown are a typical hysteresis loop (a) before and (b) after paramagnetic slope correction and (c) the Day plot [*Day et al.*, 1977]. Abbreviations are $H_c$, coercivity; $H_{cr}$, coercivity of remanence; $M_{rs}$, saturation remanence; $M_s$, saturation magnetization; SD, single domain; PSD, pseudo single domain; MD, multidomain; SP, superparamagnetic. Also shown are mixture models (SD-SP and SD-MD) and SP saturation envelope from *Dunlop* [2002].

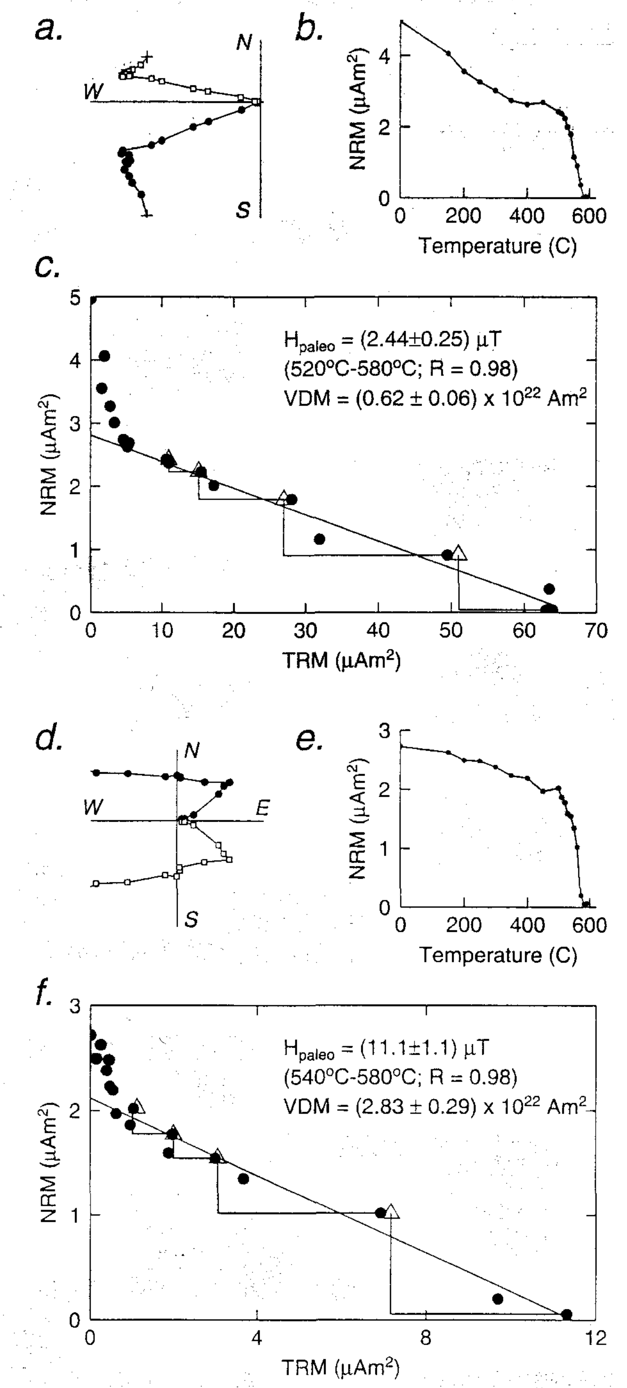


**Figure 5.** Thellier paleointensity determinations on whole rock samples from the dikes (a–c) MC15 and (d–f) MC19. Figures 5a and 5d show orthogonal vector plots of field-off steps (vertical projection of NRM, open squares; horizontal projection of NRM, closed circles). Figures 5b and 5e show natural remanent magnetization (NRM) lost versus temperature. Figures 5c and 5f show NRM lost versus partial thermoremanent magnetization gained (solid circles). Triangles are partial TRM checks.

glass (SBG) from three Pacific basin sites [*Smirnov and Tarduno*, 2003] showed $M_s$ increases at heating temperatures as low as 250°C. Moreover, the total $M_s$ increase of the SBG after all Thellier heatings was sometimes greater by a factor of 4. Therefore, while there are some changes in the magnetic hysteresis parameters of the Matachewan dike monitor samples with heating, these are relatively minor compared to cases with demonstrable experimentally induced alteration.

[35] To further investigate potential alteration induced by heating, we applied the first-order reversal curve (FORC) technique [e.g., *Pike et al.*, 1999]. Compared to traditional hysteresis measurements, the FORC method may provide additional insight into magnetic interactions and grain size distributions [*Roberts et al.*, 2000].

[36] We measured FORC diagrams for two samples from the same field-drilled core; one sample was fresh, the other was heated in the paleointensity experiment (Figure 7). The FORC diagram for the fresh sample (Figure 7a) is consistent with those reported for synthetic and natural PSD samples [e.g., *Roberts et al.*, 2000; *Muxworthy and Dunlop*, 2002]. The multiple heatings of the Thellier experiment result in a somewhat broader FORC distribution, but its overall shape remains the same (Figure 7b). This broadening may indicate a higher concentration of defects due to either maghemitization or reversion of the magnetite-ilmenite intergrowths to titanomagnetite.

### 4.3. Cooling Rate Correction

[37] A difference in cooling rate between the natural remanence and laboratory pTRM acquisitions may result in an overestimation [e.g., *Dodson and McClelland-Brown*, 1980; *Halgedahl et al.*, 1980] or underestimation [*McClelland-Brown*, 1984] of paleointensity for rocks containing SD or MD magnetic carriers, respectively.

[38] We used a conductive cooling model [*Turcotte and Schubert*, 1982] to calculate the time required for the dikes MC-15 (22.4 meter width) and MC-19 (29.2 meter width) to cool from 580°C to 500°C (approximately the maximum and minimum laboratory unblocking temperatures of our samples). Assuming that 1200°C magma intruded a 20°C country rock in a single event, the time was found to be ~6 years for dike MC-15 and ~10 years for dike MC-19.

[39] Intrusion into a preheated country rock may significantly reduce the cooling rate. For example, for intrusion

**Table 1.** Thellier Paleointensity Results From Whole Rock Samples[a]

| Sample | TR, °C | $H_a$, μT | $N$ | $b$ | $\sigma_b$ | $f$ | $g$ | $q$ |
|---|---|---|---|---|---|---|---|---|
| mc15-1 | 540–580 | 2.11 | 5 | −0.035 | 0.003 | 0.429 | 0.648 | 3.42 |
| mc15-2 | 510–570 | 2.06 | 7 | −0.034 | 0.002 | 0.468 | 0.813 | 5.88 |
| mc15-3 | 520–570 | 1.91 | 6 | −0.032 | 0.004 | 0.760 | 0.678 | 4.03 |
| mc15-4 | 530–580 | 2.08 | 6 | −.035 | 0.003 | 0.728 | 0.603 | 5.62 |
| mc15-5 | 520–580 | 2.44 | 7 | −0.041 | 0.004 | 0.748 | 0.803 | 5.93 |
| mc15-6 | 530–570 | 2.26 | 5 | −0.038 | 0.003 | 0.648 | 0.600 | 4.96 |
| mc19-1 | 540–580 | 9.99 | 5 | −0.166 | 0.007 | 0.614 | 0.436 | 6.44 |
| mc19-2 | 540–580 | 7.46 | 5 | −0.124 | 0.006 | 0.604 | 0.638 | 8.13 |
| mc19-3 | 510–560 | 11.86 | 6 | −0.198 | 0.018 | 0.442 | 0.723 | 3.61 |
| mc19-4 | 540–580 | 11.13 | 5 | −0.185 | 0.019 | 0.715 | 0.680 | 4.68 |
| mc19-5 | 530–570 | 8.40 | 5 | −0.140 | 0.026 | 0.652 | 0.728 | 2.53 |
| mc19-6 | 520–580 | 10.07 | 7 | −0.168 | 0.014 | 0.763 | 0.747 | 6.72 |

[a]Shown are the temperature range (TR) used for paleointensity determination, paleofield value ($H_a$), number of temperature steps used in line fit ($N$), slope of the line fit ($b$), the standard error of the slope ($\sigma_b$), fraction of NRM used for paleointensity determination ($f$), gap factor ($g$), and quality factor ($q$). The parameters $b$, $\sigma_b$, $f$, $g$, and $q$ were calculated after *Coe et al.* [1978].

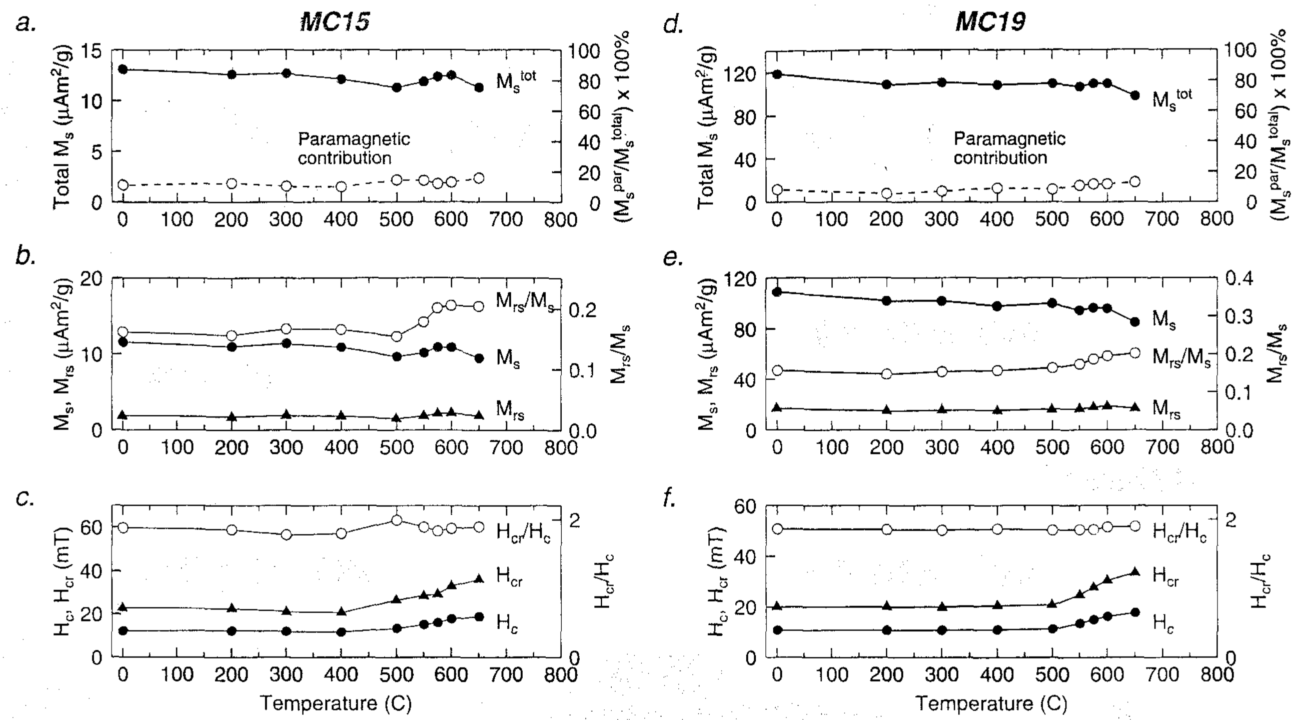

**Figure 6.** Magnetic hysteresis parameters measured at room temperature as a function of heating temperature for two of the "monitor" whole rock samples (see text) (a–c) MC15 and (d–e) MC19. Figures 6a and 6d show the total saturation magnetization ($M_s^{total}$) before slope correction (solid circles and solid line). Paramagnetic contribution ($M_s^{par}$) is the difference between $M_s^{total}$ and the saturation magnetization ($M_s$) after slope correction, normalized to $M_s^{total}$ (open circles and dashed line). Figures 6b and 6e show saturation magnetization ($M_s$) after slope correction (solid circles), saturation remanent magnetization ($M_{rs}$, solid triangles), and the $M_{rs}/M_s$ ratio (open circles). Figures 6c and 6f show coercivity ($H_c$, solid circles), coercivity of remanence ($H_{cr}$, solid triangles), and the $H_{cr}/H_c$ ratio (open circles).

into a 300°C country rock, the calculated cooling times for dikes MC-15 and MC-19 are ~42 and ~72 years, respectively.

[40] There is as yet no firm indication of the temperature of the country rocks at the time of Matachewan dike intrusion. However, the variable presence of clouded feldspar [*Halls and Zhang*, 1998] suggests that areas outside of the KSZ, such as those we have sampled, may also represent crustal levels that were at elevated temperatures during dike intrusion.

[41] If our rocks contained SD magnetic grains and the dikes were intruded into hot crust as discussed above, our Thellier data could overestimate the true field by ~25% [*Halgedahl et al.*, 1980]. The actual overestimate, however, is probably much lower because our rocks contain PSD rather than SD magnetic grains.

## 5. Discussion

[42] The low paleointensity values we have obtained are similar to those reported for the Matachewan dikes by other authors. In a Thellier study employing a special oven allowing precise temperature control and very small temperature steps, *Macouin et al.* [2003] derived a mean VDM value of 2.80 ± 0.87 × $10^{22}$ $Am^2$ from five sites (26 individual determinations). *Halls et al.* [2004] used the

**Table 2.** Magnetic Hysteresis Parameters Measured at Room Temperature From a Fresh Sample and After Heating to 600°C for the "Monitor" Samples Used During Paleointensity Determination (See Text)[a]

| | $M_s$, $\mu Am^2/g$ | | $M_{rs}/M_s$ | | $H_c$, mT | | $H_{cr}$, mT | | $H_{cr}/H_c$ | |
|---|---|---|---|---|---|---|---|---|---|---|
| Sample | Fresh | Heated | Fresh | Heated | Fresh | Heated | Fresh | Heated | Fresh | Heated |
| MC15-1 | 11.6 | 10.9 | 0.161 | 0.205 | 12.2 | 17.7 | 22.9 | 33.1 | 1.88 | 1.87 |
| MC15-2 | 3.05 | 3.29 | 0.163 | 0.189 | 11.8 | 18.5 | 21.5 | 37.6 | 1.82 | 2.03 |
| MC15-3 | 9.11 | 9.15 | 0.167 | 0.202 | 12.0 | 18.1 | 22.2 | 36.0 | 1.85 | 1.99 |
| MC19-1 | 10.9 | 9.61 | 0.157 | 0.195 | 10.8 | 16.2 | 20.1 | 30.6 | 1.86 | 1.89 |
| MC19-2 | 9.54 | 9.11 | 0.151 | 0.184 | 11.3 | 17.0 | 19.7 | 28.3 | 1.74 | 1.66 |
| MC19-3 | 8.87 | 8.94 | 0.159 | 0.191 | 12.1 | 15.5 | 21.7 | 28.5 | 1.79 | 1.84 |

[a]Shown are $H_c$, coercivity; $H_{cr}$, coercivity of remanence; $M_{rs}$, saturation remanence; and $M_s$, saturation magnetization.

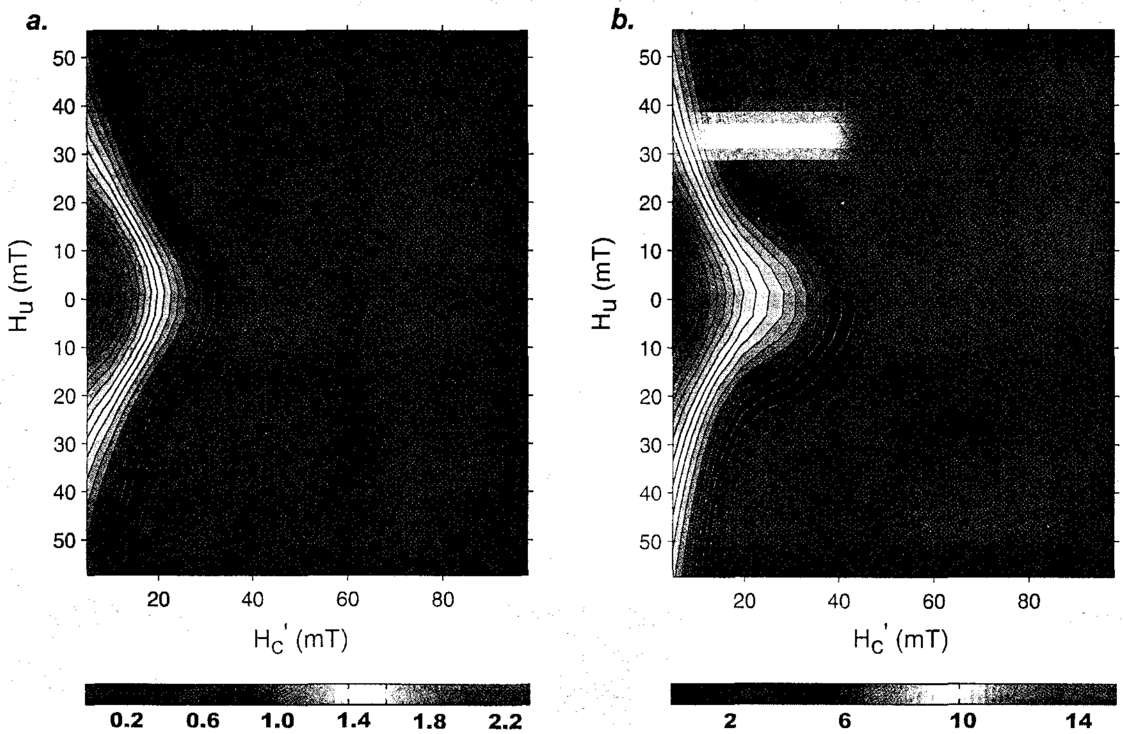


**Figure 7.** First-order reversal curve (FORC) diagrams [*Pike et al.*, 1999] measured from (a) a fresh sample and (b) a sample heated in the Thellier paleointensity experiment. Measurement of a FORC begins by saturating a sample with a large positive magnetic field. Then the field is decreased to a reversal field $H_a$, and the FORC is defined by the partial hysteresis curve that results when the applied field is increased from $H_a$ back to saturation. This measurement procedure is repeated for different values of $H_a$ to obtain a set of FORCs. The magnetization at the applied field $H_b$ on the FORC with reversal point $H_a$ is denoted by $M(H_a, H_b)$, where $H_b \geq H_a$. The FORC distribution is defined as $\rho(H_a, H_b) \equiv -\partial^2 M(H_a,$ $-\partial^2 M(H_a, H_b)/\partial H_a \partial H_b$ [*Pike et al.*, 1999; *Roberts et al.*, 2000]. For convenience during plotting, the FORC diagram axes are usually rotated by changing coordinates from $\{H_a, H_b\}$ to $H_c' = (H_b - H_a)/2$ and $H_u = (H_b + H_a)/2$. The color legends below the FORC diagrams show the density of FORC distribution $\rho(H_a, H_b)$. The smoothing factor is 5.

microwave technique [e.g., *Shaw et al.*, 1996] to obtain a mean VDM value of $2.53 \pm 0.93 \times 10^{22}$ Am$^2$ from twelve Matachewan dikes. *McArdle et al.* [2004] reported similar VDM values from four Matachewan dikes.

[43] Paleomagnetic directions from our dikes, when compared to reference poles [*Bates and Halls*, 1990] indicate that our paleointensities reflect the stable nontransitional field. However, our observed VDM values are less than the transitional VDM values that characterize transitions or excursions in 0.03–10 Ma volcanic rocks [*Tanaka et al.*, 1995]. Therefore, taken at face value, our whole rock results support a very low field intensity in the Early Proterozoic.

[44] However, the directional data from the Matachewan dikes, together with data from Karelia and the Pilbara craton [*Mertanen et al.*, 1999; *Strik et al.*, 2003], suggest that the latitudinal variation of secular variation in Late Archean–Early Proterozoic times was strikingly similar to that of the last 5 million years. The only difference seems to be that the Archean–Early Proterozoic data hint at a smaller contribution of the quadrupole family to the field [*Smirnov and Tarduno*, 2004].

[45] The overall similarity between the geomagnetic field in the Late Archean–Early Proterozoic with the more recent field does not in itself exclude a very weak field such as that implied by our paleointensity data and that of others derived from Matachewan dike whole rock samples. In fact, if it could be established that PSV was nearly constant while there were very large changes in mean field strength, we would have another important constraint on how the dynamo operates on long timescales. However, other paleointensity values from Archean-Proterozoic dikes [*Yoshihara and Hamano*, 2000] and single plagioclase crystals [*Smirnov et al.*, 2003] raise some questions, as they yield values that are more consistent with the modern field. Therefore it is prudent to examine our data to exclude potential factors that might grossly violate requirements of the Thellier approach.

[46] In our case, experimental alteration is unlikely to introduce a large spurious signal. Indeed, the magnetic hysteresis monitoring experiments (Figure 6) show that magnetic alteration is minor. This is further supported by the data of *Macouin et al.* [2003], who imparted a total TRM to the samples used in paleointensity experiments and were able to retrieve the laboratory field value. These results also indicate that the effects of pTRM tails due to MD grains [e.g., *Shcherbakova and Shcherbakov*, 2000] are negligible in the Matachewan dikes.

[47] Relatively low $M_{rs}/M_s$ ratios observed from the Matachewan dikes we have sampled, taken at face value, suggest that the magnetic grains are in the vortex state

[*Williams and Dunlop*, 1995]. On the basis of a micromagnetic model, *Winklhofer et al.* [1997] proposed that grains in the vortex state could result in paleointensity underestimates because they will behave as SD grains on laboratory timescales, and as PSD grains on geological timescales. However, the applicability of this model to natural rocks (especially those with oxyexsolution structures) is unknown. It is premature to use the $M_{rs}/M_s$ ratio to assign a vortex state to the magnetite grains of the Matachewan dikes because of the important roles of shape anisotropy and the crystallographic orientation of the magnetite intergrowths.

[48] Because of high unblocking temperatures of the ChRM, and its dominant pseudo single domain state, remagnetization during the geological life of the Matachewan rocks is also unlikely [*Dunlop and Buchan*, 1977]; no geological events have been reported which could have resulted in such a remagnetization. However, to yield a reliable paleointensity value, the Matachewan dikes must record a TRM, and our SEM data, prior examples of oxyexsolution below 500°C, and rock magnetic calculations, indicate this may not be the case.

### 5.1. High-Temperature Oxidation

[49] Magnetic grains in dolerites crystallize as a magnetite-ülvospinel solid solution (titanomagnetite):

$$(1-x)Fe_3O_4 \cdot xFe_2TiO_4 \tag{1}$$

where $x$ is Ti content [*Buddington and Lindsley*, 1964; *Frost*, 1991]. Very rapid cooling preserves titanomagnetite in solid solution at room temperature [*Ozima and Larson*, 1970]. Slow cooling in reducing conditions may assist the preservation of $Fe_2TiO_4$ in solid solution down to the magnetite-ülvospinel solvus, resulting in exsolution of a ülvospinel-rich phase in the host magnetite [e.g., *Lindsley*, 1981]. However, under oxidizing conditions, titanomagnetite may be oxidized to produce intergrowths of magnetite with ilmenite lamellae [e.g., *Buddington and Lindsley*, 1964; *Frost and Lindsley*, 1991]. This process is termed oxyexsolution.

[50] With continued oxidation, the magnetite-ilmenite intergrowths evolve to mixtures of hematite, pseudobrookite, and rutile [*Buddington and Lindsley*, 1964]. The resulting oxide assemblage may vary depending on oxygen fugacity, temperature, cooling rate, and initial composition. Our SEM and rock magnetic analyses, however, show that in our samples the oxyexsolution has advanced only to stage C3 (abundant ilmenite lamellae; equilibrium two-phase intergrowths) of *Wilson and Watkins* [1967] and *Haggerty* [1991].

[51] Magnetite-ilmenite intergrowths have been observed in a wide range of rocks [e.g., *Schwarz and Symons*, 1970; *Kono et al.*, 1980; *Hodych*, 1996; *Kosterov*, 2001]. The presence of such intergrowths is usually associated with a highly stable ChRM [e.g., *Larson et al.*, 1969; *Tucker and O'Reilly*, 1980]. However, the nature of this magnetization is defined by the temperature at which the oxyexsolution ceases during initial cooling. A pure TRM is acquired only if oxyexsolution stops above the Curie point of a given magnetic phase. Otherwise, the remanence is a thermochemical remanent magnetization (TCRM), produced by simultaneous slow cooling and volume growth of a magnetic phase below its Curie temperature [*Nagata and Kobayashi*, 1963; *Dunlop and Özdemir*, 1997].

[52] The formation of TCRM may be a common process in nature [e.g., *Kellogg et al.*, 1970; *Dunlop and Özdemir*, 1997]. Equilibrium temperatures of many oxidized assemblages in basaltic lavas can be as low as 600°C [*Carmichael and Nicholls*, 1967]. In cooling lava lakes, however, the oxyexsolution of titanomagnetite was observed to continue 100–400°C below equilibrium temperatures. For example, the formation of magnetite was observed at temperatures as low as 500°C [*Grommé et al.*, 1969]. Intergrowths of thin ilmenite lamellae found in magnetite from orthogneisses developed in rocks of the amphibolite facies further suggest that high-temperature oxidation might extend to temperature as low as 500°C [*Buddington and Lindsley*, 1964]. Even lower temperatures of oxyexsolution (<500°C) are suggested by low oxygen closure temperatures observed in the Fe-Ti oxide–rich troctolite from the Laramie anorthosite complex [*Farquhar and Chacko*, 1994].

[53] Unfortunately, experimental and theoretical estimates of the temperature at which oxyexsolution ceases are rare. Oxyexsolution was reproduced experimentally at temperatures as low as 550°C [*Buddington and Lindsley*, 1964]. The experiment was not continued to lower temperatures, but there was no indication that the process could not continue below 550°C (D. Lindsley, written communication, 2004).

[54] *Frost and Chacko* [1989] used the compositions of the intergrown phases to estimate the temperatures and oxygen fugacities at which the oxyexsolution ceased in various granulites. They found the "freezing" temperature to be between 350° and 500°C. In spite of large uncertainties associated with extrapolating values well outside the range of experimental calibration, these results suggest that oxyexsolution can continue well below the Curie temperature of magnetite.

[55] While we have no means to estimate the cessation temperature of oxyexsolution in our samples, we hypothesize that this process continued below 580°C. Consequently, the high-temperature ChRM can be a TCRM. Such a hypothesis is consistent with the fact that no pseudobrookite (which can form only at temperatures >585°C) has been identified in our samples in SEM analyses.

### 5.2. TCRM/TRM Efficiency

[56] Can a TCRM acquired during cooling accurately record field values? From theory, it follows that TCRM and TRM intensities should differ. TCRM is a special case of crystallization remanent magnetization (CRM). The CRM is blocked when a grain volume reaches a stable blocking volume $V_B$ [e.g., *Kobayashi*, 1962] for a given temperature $T$:

$$V_B = \frac{2kT \ln(2t/\tau_o)}{\mu_o M_s H_K} \tag{2}$$

where $M_s$ is the spontaneous magnetization, $\mu_o$ is the permeability of free space ($4\pi \times 10^{-7}$ $H$/m), $H_K$ is the microcoercivity of a grain, $k$ is Boltzmann's constant ($1.38 \times 10^{-23}$ J/K), $t$ is characteristic time of experiment, and $\tau_o$ is the atomic reorganization time.

[57] Assuming that the final grain size is identical and the characteristic relaxation times for TRM and CRM are comparable, *Stacey and Banerjee* [1974] obtained a theoretical expression for the CRM/TRM ratio:

$$\frac{CRM}{TRM} = \frac{H_K(T_B)}{H_K(T)} = \frac{K(T_B)}{K(T)}\left(\frac{M_s(T)}{M_s(T_B)}\right) \tag{3}$$

where $T$ is the temperature at which CRM is acquired, $T_B$ is the blocking temperature of the magnetic grains, and $K$ is an anisotropy constant.

[58] Equation (3) predicts that CRM should always be smaller than TRM. This prediction has been confirmed by experiment by *Stokking and Tauxe* [1990], who grew single-domain hematite and goethite at 95°C. The experimental CRM/TRM ratios were found to be even smaller than the value of 0.4 quoted by *Stacey and Banerjee* [1974].

[59] *McClelland* [1996] further considered the scenario when grains grow to various sizes. The author predicted that the CRM/TRM ratio may vary between 2 and 0.2 depending on the difference in timescale of acquisition of CRM and TRM, and on the blocking temperature of the grains formed. According to *McClelland*'s [1996] calculations, a CRM acquired over laboratory timescale should always be smaller than a laboratory TRM. In contrast, for a CRM formed over a longer time interval, the CRM/TRM ratio is greater than unity in the low blocking temperature range, but much smaller than unity for grains with high $T_B$. For example, for $T_B$ = 555°C, the ratio of CRM imparted at 100°C over $10^5$ years to TRM was predicted to be 0.337.

[60] We note, however, that the temperatures used in the CRM experiments [*Stokking and Tauxe*, 1990] and modeling [*McClelland*, 1996] are significantly lower than the temperature of TCRM acquisition we propose. Therefore they may only be considered as approximate analogues of high-temperature processes.

[61] *McClelland* [1996] proposed that for a sample dominated by high blocking temperature grains, the total remanence will be dominated by the contribution from these high $T_B$ grains. Therefore Thellier analysis of such a sample can yield apparently smaller values than the actual field intensities [e.g., *Yoshihara and Hamano*, 2004]. We note that for samples characterized by a narrow blocking temperature interval (such as our samples), the CRM/TRM ratio can be considered constant (no deviation from the linearity of the Arai plot is expected) and can be described by equation (3).

[62] Both the models of *Stacey and Banerjee* [1974] and *McClelland* [1996] are valid for an ensemble of noninteracting SD grains [e.g., *Néel*, 1955] and may not be directly applicable in the case of larger grains. However, *McClelland* [1996] argued that as long as the CRM is thermally activated, both CRM and TRM should follow the same relationships, although numerical values can be different.

[63] Some rough estimates of the TCRM/TRM ratio for PSD grains can be obtained from experimental data. First, we note that the theoretical CRM/TRM ratio for CRM imparted at 300°C over $10^5$ sec in the SD ensemble with $T_B$ = 565°C (0.683) [*McClelland*, 1996] is higher than the experimentally determined ratio (0.166) for PSD (0.2 to 3.0 μm) magnetite [*Pucher*, 1969]. Therefore, for samples characterized by high $T_B$ in a narrow range, the estimates obtained for SD magnetite may represent an upper limit for the CRM/TRM ratio.

[64] Equation (3) allows us to use an experimental temperature dependence of the coercivity, $H_c(T)$ to approximate the TCRM/TRM ratio for our samples. We utilize the $H_c(T)$ dependence determined for PSD magnetite using FORC diagrams [*Muxworthy and Dunlop*, 2002]. We select a grain size (1.7 μm) closest to that of the magnetite intergrowths we observed in our SEM analyses. Assuming that the proportionality between $H_c$ and $H_K$ is temperature-independent, the effective temperature of TCRM acquisition is 500°C and $T_B$ is 570°C, we obtain the TCRM/TRM ratio of ~0.25.

[65] In detail, the TCRM effect will depend on the history of oxyexsolution. The bias we calculate above will be greatest when grain growth above the Curie temperature of magnetite is restricted to superparamagnetic (SP) grain sizes, which then grow through the SP-SD threshold at lower temperatures. This might be the case of the Matachewan dikes, which probably underwent an initial rapid phase of cooling, followed by slower cooling as they came into equilibrium with the warm crust into which they were injected.

[66] Alternatively, if some grains grow through the SP/SD threshold above 580°C, they could carry a true TRM. In this case the NRM would be a mixture of TRM and TCRM, reducing the low-field bias. However, this scenario assumes independence of magnetic grain growth above and below 580°C. Grains originally formed above 580°C will probably continue to grow by diffusion at lower temperatures, and their magnetizations could be reset. In this case, the true blocking temperature may in fact be close to the temperature at which grain growth ceases. Future studies of magnetic grain growth may resolve this issue.

### 5.3. TCRM and the Precambrian Field

[67] The TCRM/TRM efficiency value above suggests that Thellier paleointensity values such as those we report could underestimate the true field strength by a factor of four (or more). This uncertainty in TRM fidelity translates into a potential range of field values that spans that defined by the modern field (~8 × $10^{22}$ Am$^2$) and proposed low Precambrian levels (~2 × $10^{22}$ Am$^2$). In light of these uncertainties we feel it is premature to conclude the Precambrian field was weak based on paleointensity data from the Matachewan dikes.

[68] Other Precambrian (and Phanerozoic rocks) may carry TCRMs. This issue was highlighted by *Dunlop and Özdemir* [1997] who stated: "The NRM of subaerial basalts has long been taken to be TRM par excellence. But is this really true?" In our opinion, understanding further how TCRM is acquired and records the field is a major challenge for the use of many rocks in defining the strength of the Precambrian field.

[69] Finally, we note that excluding the case of exceptionally thick dikes (i.e., those over ≫50 m in thickness), the presence of TCRM should not adversely affect the fidelity of paleomagnetic directional records. In most dikes and lavas TCRM will be acquired after cooling

on timescales that are still much shorter than hundreds of years.

## 6. Conclusions

[70] One of the basic assumptions underlying the Thellier method for paleointensity determination is that the paleointensity signal is carried by a thermal remanent magnetization. Testing the veracity of this assumption is in turn a crucial part of paleointensity analysis. If the characteristic remanence is a thermochemical remanent magnetization acquired below the Curie point of magnetite, paleointensity data may lead to the derivation of field values that are too low. This is a particularly pertinent issue in the case of Precambrian dikes that may have been intruded into crust with elevated temperatures. It is not possible to identify the paleointensity bias using standard reliability criteria based on the characteristics of natural remanent magnetizations, and thermal remanent magnetizations imparted in the laboratory. Instead the magnetic mineralogy must be first scrutinized to determine whether the telltale signs of thermochemical remanence are present. Understanding the temperature range at which oxyexsolution occurs, as well as better constraining the efficiency of thermochemical remanence, are major prerequisites for the use of many Precambrian rocks as absolute paleointensity recorders.

[71] **Acknowledgments.** We thank Peter Lippert for taking part in sampling the Matachewan dikes and Pavel Doubrovine for help with paleomagnetic and SEM measurements. We are grateful to Robert Coe, Peter Riisager, and the associate editor for their reviews of the manuscript. This research was supported by the National Science Foundation.

## References

Anderson, D. L. (2003), Look again, *Astron. Geophys.*, *44*, 10–12.
Bates, M. P., and H. C. Halls (1990), Regional variation in paleomagnetic polarity of the Matachewan dyke swarm related to the Kapuskasing structural zone, Ontario, *Can. J. Earth Sci.*, *27*, 200–211.
Bates, M. P., and H. C. Halls (1991), Broad-scale Proterozoic deformation of the central Superior Province revealed by paleomagnetism of the 2.45 Ga Matachewan dyke swarm, *Can. J. Earth Sci.*, *28*, 1780–1796.
Bogatikov, O. A., O. V. Karpova, D. M. Pecherskiy, and Z. V. Sharonova (1971), Homogenization of titanomagnetites and reconstruction of the composition of primary titanomagnetite, *Phys. Solid Earth*, *7*, 498–505.
Breuer, D., and T. Spohn (1995), Possible flush instability in mantle convection at the Archaean-Proterozoic transition, *Nature*, *378*, 608–610.
Brodholt, J., and F. Nimmo (2002), Core values, *Nature*, *418*, 489–491.
Buddington, A. F., and D. H. Lindsley (1964), Iron-titanium oxide minerals and synthetic equivalents, *J. Petrol.*, *5*, 310–357.
Calvo, M., M. Prévot, M. Perrin, and J. Riisager (2002), Investigating the reason for the failure of paleointensity experiments: A study on historical lava flows from Mt. Etna (Italy), *Geophys. J. Int.*, *149*, 44–63.
Carmichael, I. S. E., and J. Nicholls (1967), Iron-titanium oxides and oxygen fugacities in volcanic rocks, *J. Geophys. Res.*, *72*, 4665–4687.
Clark, D. A., and P. W. Schmidt (1982), Theoretical analysis of thermomagnetic properties, low-temperature hysteresis and domain structure of titanomagnetites, *Phys. Earth Planet. Inter.*, *30*, 300–316.
Coe, R. S. (1967), Paleointensities of Earth's magnetic field determined from Tertiary and Quaternary rocks, *J. Geophys. Res.*, *72*, 3247–3262.
Coe, R. S., S. Gromme, and E. A. Mankinen (1978), Geomagnetic paleointensities from radiocarbon dates lava flows on Hawaii and the question of the Pacific non-dipole low, *J. Geophys. Res.*, *83*, 1059–1069.
Condie, K. C., D. J. Bobrow, and K. D. Card (1987), Geochemistry of Precambrian mafic dykes from the southern Superior Province of the Canadian Shield, in *Mafic Dyke Swarms*, edited by H. C. Halls and W. F. Fahrig, *Geol. Soc. Can. Spec. Pap.*, *34*, 95–108.
Cottrell, R. D., and J. A. Tarduno (2000), In search of high fidelity paleointensities: A comparison of single crystal and whole rock Thellier-Thellier analyses, *J. Geophys. Res.*, *105*, 23,579–23,594.
Day, R., M. Fuller, and V. A. Schmidt (1977), Hysteresis properties of titanomagnetites: Grain-size and compositional dependence, *Phys. Earth Planet. Inter.*, *13*, 260–267.
Dodson, M., and E. McClelland-Brown (1980), Magnetic blocking temperatures of single-domain grains during slow cooling, *J. Geophys. Res.*, *85*, 2625–2637.
Dunlop, D. J. (1974), Thermal enhancement of magnetic susceptibility, *J. Geophys.*, *40*, 439–451.
Dunlop, D. J. (2002), Theory and application of the Day plot ($M_{rs}/M_s$ versus $H_{cr}/H_c$): 1. Theoretical curves and tests using titanomagnetite data, *J. Geophys. Res.*, *107*(B3), 2056, doi:10.1029/2001JB000486.
Dunlop, D. J., and K. L. Buchan (1977), Thermal remagnetization and paleointensity record of metamorphic rocks, *Phys. Earth Planet. Inter.*, *13*, 325–331.
Dunlop, D. J., and Ö. Özdemir (1997), *Rock Magnetism: Fundamentals and Frontiers*, 573 pp., Cambridge Univ. Press, New York.
Ernst, R. E., and H. C. Halls (1984), Paleomagnetism of the Hearst dike swarm and implications for the tectonic history of the Kapuskasing structural zone, northern Ontario, *Can. J. Earth Sci.*, *21*, 1499–1506.
Fahrig, W. F. (1987), The tectonic settings of continental mafic dyke swarms: Failed arm and early passive margin, in *Mafic Dyke Swarms*, edited by H. C. Halls and W. F. Fahrig, *Geol. Soc. Can. Spec. Pap.*, *34*, 331–348.
Farquhar, J., and T. Chacko (1994), Exsolution-enhanced oxygen exchange: Implications for oxygen isotope closure in minerals, *Geology*, *22*, 751–754.
Foulger, G. R., and J. H. Natland (2003), Is "hotspot" volcanism a consequence of plate tectonics?, *Science*, *300*, 921–922.
Frost, B. R. (1991), Magnetic petrology: Factors that control the occurence of magnetite in crustal rocks, *Rev. Mineral.*, *25*, 489–509.
Frost, B. R., and T. Chacko (1989), The granulite uncertainty principle: Limitations on thermobarometry in granulites, *J. Geol.*, *97*, 435–450.
Frost, B. R., and D. H. Lindsley (1991), Occurrence of iron-titanium oxides in igneous rocks, *Rev. Mineral.*, *25*, 434–468.
Goldstein, J. I., D. E. Newbury, P. Echlin, D. C. Joy, A. D. Romig Jr., C. E. Lyman, C. Fiori, and E. Lifshin (1992), *Scanning Electron Microscopy and X-Ray Microanalysis*, 820 pp., Springer, New York.
Grommé, C. S., T. L. Wright, and D. L. Peck (1969), Magnetic properties and oxidation of iron-titanium oxide minerals in Alae and Makaopuhi lava lakes, *J. Geophys. Res.*, *74*, 5277–5293.
Haag, M., J. R. Dunn, and M. Fuller (1995), A new quality check for absolute palaeointensities of the Earth magnetic field, *Geophys. Res. Lett.*, *22*, 3549–3552.
Haggerty, S. E. (1991), Oxide textures—A mini-atlas, *Rev. Mineral.*, *25*, 129–219.
Hale, C. J. (1987), The intensity of the geomagnetic field at 3.5 Ga: Paleointensity results from the Komati formation, Barberton Mountain Land, South Africa, *Earth Planet. Sci. Lett.*, *86*, 354–364.
Halgedahl, S., R. Day, and M. Fuller (1980), The effect of cooling rate on the intensity of weak-field TRM in single-domain magnetite, *J. Geophys. Res.*, *85*, 3690–3698.
Halls, H. C. (1991), The Matachewan dyke swarm, Canada: An early Proterozoic magnetic field reversal, *Earth Planet. Sci. Lett.*, *105*, 279–292.
Halls, H. C. (1998), Global mafic magmatism at 2.5 Ga: Remnants of an ancient large igneous province? (Comment), *Geology*, *26*, 93–94.
Halls, H. C., and M. P. Bates (1990), The evolution of 2.45 Ga Matachewan dyke swarm, Canada, in *Mafic Dykes and Emplacement Mechanisms*, edited by A. J. Parker, P. C. Rickwood, and D. H. Tucker, pp. 237–250, A. A. Balkema, Brookfield, Vt.
Halls, H. C., and H. C. Palmer (1990), The tectonic relationship of two Early Proterozoic dyke swarms to the Kapuskasing structural zone: A paleomagnetic and petrographic study, *Can. J. Earth Sci.*, *27*, 87–103.
Halls, H. C., and B. Zhang (1998), Uplift structure of the southern Kapuskasing zone from 2.45 Ga dike swarm displacement, *Geology*, *26*, 67–70.
Halls, H. C., and B. Zhang (2003), Crustal uplift in the southern Superior Province, Canada, revealed by paleomagnetism, *Tectonophysics*, *362*, 123–136.
Halls, H. C., H. C. Palmer, M. P. Bates, and W. C. Phinney (1994), Constraints on the nature of the Kapuskasing structural zone from the study of Proterozoic dyke swarms, *Can. J. Earth Sci.*, *31*, 1182–1196.
Halls, H. C., N. J. Mcardle, M. N. Gratton, M. J. Hill, and J. Shaw (2004), Microwave paleointensities from dyke chilled margins: A way to obtain long term variations in geodynamo intensity for the last three billion years, *Phys. Earth Planet. Inter.*, *147*, 183–195.
Heaman, L. M. (1997), Global mafic magmatism at 2.45 Ga: Remnants of an ancient large igneous province?, *Geology*, *25*, 299–302.
Hodych, J. P. (1996), Inferring domain state from magnetic hysteresis in high coercivity dolerites bearing magnetite with ilmenite lamellae, *Earth Planet. Sci. Lett.*, *142*, 523–533.
Hollerbach, R., and C. A. Jones (1993), Influence of the Earth's inner core on geomagnetic fluctuations and reversals, *Nature*, *365*, 541–543.

Kellogg, K., E. E. Larson, and D. E. Watson (1970), Thermochemical remanent magnetization and thermal remanent magnetization: A comparison in a basalt, *Science*, *170*, 628–630.
Kobayashi, K. (1962), Magnetization-blocking process by volume development of ferromagnetic fine particles, *J. Phys. Soc. Jpn.*, *17*, 695–698.
Kono, M., D. Clague, and E. E. Larson (1980), Fe-Ti oxide mineralogy of DSDP leg 55 basalts, *Initial Rep. Deep Sea Drill. Proj.*, *55*, 639–652.
Kosterov, A. A. (2001), Magnetic properties of subaerial basalts at low temperatures, *Earth Planets Space*, *53*, 883–892.
Labrosse, S., and M. Macouin (2003), The inner core and the geodynamo, *C. R. Geosci.*, *335*, 37–50.
Labrosse, S., J.-P. Poirier, and J.-L. Le Mouel (1997), On cooling of the Earth's core, *Phys. Earth Planet. Inter.*, *99*, 1–17.
Labrosse, S., J.-P. Poirier, and J.-L. Le Mouel (2001), The age of the inner core on geomagnetic fluctuations and reversals, *Earth Planet. Sci. Lett.*, *190*, 111–123.
Larson, E., M. Ozima, M. Ozima, T. Nagata, and D. Strangway (1969), Stability of remanent magnetization of rocks, *Geophys. J. R. Astron. Soc.*, *17*, 263–292.
Lindsley, D. H. (1981), Some experiments pertaining to the magnetite-ülvospinel miscibility gap, *Am. Mineral.*, *66*, 759–762.
Macouin, M., J. P. Valet, J. Besse, K. Buchan, R. Ernst, M. LeGoff, and U. Scharer (2003), Low paleointensities recorded in 1 to 2.4 Ga Proterozoic dykes, Superior Province, Canada, *Earth Planet. Sci. Lett.*, *213*, 79–95.
Manson, M. L., and H. C. Halls (1997), Proterozoic reactivation of the southern Superior Province and its role in the evolution of the Midcontinent rift, *Can. J. Earth Sci.*, *34*, 562–575.
McArdle, N. J., H. C. Halls, and J. Shaw (2004), Rock magnetic studies and a comparison between microwave and Thellier palaeointensities for Canadian Precambrian dykes, *Phys. Earth Planet. Inter.*, *147*, 247–254.
McClelland, E. (1996), Theory of CRM acquired by grain growth, and its implications for TRM discrimination and paleointensity determination in igneous rocks, *Geophys. J. Int.*, *126*, 271–280.
McClelland-Brown, E. (1984), Experiments on TRM intensity dependence on cooling rate, *Geophys. Res. Lett.*, *11*, 205–208.
McElhinny, M. W., and M. E. Evans (1968), An investigation of the strength of the geomagnetic field in the Early Precambrian, *Phys. Earth Planet. Inter.*, *1*, 485–497.
Mertanen, S., H. C. Halls, J. I. Vuollo, L. J. Pesonen, and V. S. Stepanov (1999), Paleomagnetism of 2.44 Ga mafic dykes in Russian Karelia, eastern Fennoscandian Shield—Implications for continental reconstructions, *Precambrian Res.*, *98*, 197–221.
Muxworthy, A. R., and D. J. Dunlop (2002), First-order reversal curve (FORC) diagrams for pseudo-single-domain magnetites at high temperature, *Earth Planet. Sci. Lett.*, *203*, 369–382.
Nagata, T., and K. Kobayashi (1963), Thermo-chemical remanent magnetization of rocks, *Nature*, *197*, 476–477.
Néel, L. (1955), Some theoretical aspects of rock magnetism, *Adv. Phys.*, *4*, 191–243.
Nelson, D. O., D. A. Morrison, and W. C. Phinney (1990), Open-system evolution versus source control in basaltic magmas: Matachewan-Hearst dike swarm, Superior Province, Canada, *Can. J. Earth Sci.*, *27*, 767–783.
Özdemir, Ö., D. J. Dunlop, and B. M. Moskowitz (1993), The effect of oxidation on the Verwey transition in magnetite, *Geophys. Res. Lett.*, *20*, 1671–1674.
Ozima, M., and E. E. Larson (1970), Low- and high-temperature oxidation of titanomagnetite in relation to irreversible changes in the magnetic properties of submarine basalts, *J. Geophys. Res.*, *75*, 1003–1017.
Phinney, W. C., and H. C. Halls (2001), Petrogenesis of the Early Proterozoic Matachewan dyke swarm, Canada, and implications for magma emplacement and subsequent deformation, *Can. J. Earth Sci.*, *38*, 1541–1563.
Pike, C. R., A. P. Roberts, and K. L. Verosub (1999), Characterizing interactions in fine magnetic particle systems using first order reversal curves, *J. Appl. Phys.*, *85*, 6660–6667.
Poldervaart, A., and A. K. Gilkey (1954), On clouded feldspars, *Am. Mineral.*, *39*, 75–91.
Pucher, R. (1969), Relative stabilities of chemical and thermal remanence in synthetic ferrites, *Earth Planet. Sci. Lett.*, *6*, 107–111.
Riisager, P., J. Riisager, X. Zhao, and R. S. Coe (2003), Cretaceous geomagnetic paleointensities: Thellier experiments on pillow lavas and submarine basaltic glass from the Ontong Java plateau, *Geochem. Geophys. Geosyst.*, *4*(12), 8803, doi:10.1029/2003GC000611.
Roberts, A. P., C. R. Pike, and K. L. Verosub (2000), FORC diagrams: A new tool for characterizing the magnetic properties of natural samples, *J. Geophys. Res.*, *105*, 28,461–28,475.
Schutts, L. D., and D. J. Dunlop (1981), Proterozoic magnetic overprinting of Archaean rocks in the Canadian Superior Province, *Nature*, *291*, 642–645.
Schwarz, E. J., and D. T. A. Symons (1970), Paleomagnetic field intensity during cooling of the Sudbury irruptive 1700 million years ago, *J. Geophys. Res.*, *75*, 6631–6640.
Selkin, P. A., J. S. Gee, L. Tauxe, W. P. Meurer, and A. J. Newell (2000), The effect of remanence anisotropy on paleointensity estimates: A case study from the Archean Stillwater Complex, *Earth Planet. Sci. Lett.*, *183*, 403–416.
Shaw, J., D. Walton, S. Yang, T. C. Rolph, and J. A. Share (1996), Microwave archaeointensities from Peruvian ceramics, *Geophys. J. Int.*, *124*, 241–244.
Shcherbakova, V. V., and V. P. Shcherbakov (2000), Properties of partial thermoremanent magnetization in pseudosingle domain and multidomain magnetite grains, *J. Geophys. Res.*, *105*, 767–781.
Sleep, N. H. (2003), Mantle plumes?, *Astron. Geophys.*, *44*, 11–13.
Smirnov, A. V., and J. A. Tarduno (2003), Magnetic hysteresis monitoring of Cretaceous submarine basaltic glass during Thellier paleointensity experiments: Evidence for alteration and attendant low field bias, *Earth Planet. Sci. Lett.*, *206*, 571–585.
Smirnov, A. V., and J. A. Tarduno (2004), Secular variation of the Late Archean–Early Proterozoic geodynamo, *Geophys. Res. Lett.*, *31*, L16607, doi:10.1029/2004GL020333.
Smirnov, A. V., J. A. Tarduno, and B. N. Pisakin (2003), Paleointensity of the early geodynamo (2.45 Ga) as recorded in Karelia: A single crystal approach, *Geology*, *31*, 415–418.
Stacey, F. D., and S. K. Banerjee (1974), *The Physical Principles of Rock Magnetism*, 195 pp., Elsevier, New York.
Stevenson, D. J., T. Spohn, and G. Schubert (1983), Magnetism and thermal evolution of the terrestrial planets, *Icarus*, *54*, 466–489.
Stokking, L. B., and L. Tauxe (1990), Properties of chemical remanence in synthetic hematite: Testing theoretical predictions, *J. Geophys. Res.*, *95*, 12,639–12,652.
Strik, G., T. S. Blake, T. E. Zegers, S. H. White, and C. G. Langereis (2003), Palaeomagnetism of flood basalts in the Pilbara Craton, Western Australia: Late Archaean continental drift and the oldest known reversal of the geomagnetic field, *J. Geophys. Res.*, *108*(B12), 2551, doi:10.1029/2003JB002475.
Symons, D. T. A., M. T. Lewchuk, D. J. Dunlop, V. Costanzo-Alvarez, H. C. Halls, M. P. Bates, H. C. Palmer, and T. A. Vandall (1994), Synopis of paleomagnetic studies in the Kapuskasing structural zone, *Can. J. Earth Sci.*, *31*, 1206–1217.
Tanaka, H., and M. Kono (1991), Preliminary results and reliability of paleointensity studies on historical and $^{14}C$ dated Hawaiian lavas, *J. Geomagn. Geoelectr.*, *43*, 375–388.
Tanaka, H., M. Kono, and H. Uchimura (1995), Some global features of palaeointensity in geological time, *Geophys. J. Int.*, *120*, 97–102.
Thellier, E., and O. Thellier (1959), Sur l'intensité du champ magnétique terrestre dans le passé historique et géologique, *Ann. Geophys.*, *15*, 285–376.
Tucker, P., and W. O'Reilly (1980), The laboratory simulation of deuteric oxidation of titanomagnetites: Effect on magnetic properties and stability of thermoremanence, *Phys. Earth Planet. Inter.*, *23*, 112–133.
Turcotte, D. L., and G. Schubert (1982), *Geodynamics: Applications of Continuum Physics to Geological Problems*, 450 pp., John Wiley, Hoboken, N. J.
Wicht, J. (2002), Inner-core conductivity in numerical dynamo simulations, *Phys. Earth Planet. Inter.*, *132*, 281–302.
Williams, W., and D. J. Dunlop (1995), Simulation of magnetic hysteresis in pseudo-single-domain grains of magnetite, *J. Geophys. Res.*, *100*, 3859–3871.
Wilson, R. L., and N. D. Watkins (1967), Correlation of petrology and natural magnetic polarity in Columbia Plateau basalts, *Geophys. J. R. Astron. Soc.*, *12*, 405–424.
Winklhofer, M., K. Fabian, and F. Heider (1997), Magnetic blocking temperatures of magnetite calculated with a three-dimensional micromagnetic model, *J. Geophys. Res.*, *102*, 22,695–22,709.
Yamamoto, Y., H. Tsunakawa, and H. Shibuya (2003), Palaeointensity study of the Hawaiian 1960 lava: Implications for possible causes of erroneously high intensities, *Geophys. J. Int.*, *153*, 263–276.
Yoshihara, A., and Y. Hamano (2000), Intensity of the Earth's magnetic field in late Archean obtained from diabase dikes of the Slave Province, Canada, *Phys. Earth Planet. Inter.*, *117*, 295–307.
Yoshihara, A., and Y. Hamano (2004), Paleomagnetic constraints on the Archean geomagnetic field intensity obtained from komatiites of the Barberton and Belingwe greenstone belts, South Africa and Zimbabwe, *Precambrian Res.*, *131*, 111–142.
Yu, Y. J., and D. J. Dunlop (2002), Multivectorial paleointensity determination from the Cordova Gabbro, southern Ontario, *Earth Planet. Sci. Lett.*, *203*, 983–998.

---

A. V. Smirnov and J. A. Tarduno, Department of Earth and Environmental Sciences, University of Rochester, Hutchison Hall 227, Rochester, NY 14627, USA. (alexei@earth.rochester.edu)